Published in IET Generation, Transmission & Distribution
Received on 4th February 2008
Revised on 18th April 2008
doi: 10.1049/iet-gtd:20080064

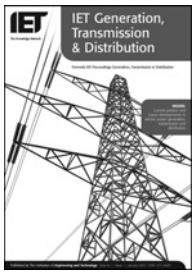

ISSN 1751-8687

OPF-based security redispatching including FACTS devices

R. Zárate-Miñano A.J. Conejo F. Milano

Department of Electrical Engineering, University of Castilla-La Mancha, Campus Universitario, s/n, 13071 Ciudad Real, Spain
E-mail: fmilano@ind-cr.uclm.es

Abstract: An Optimal Power Flow (OPF)-based security-driven redispatching procedure to archive an appropriate security level is provided. The proposed procedure is particularly suited for security redispatching by an independent system operator. This procedure uses full ac equations and explicitly considers security limits through a stressed loading condition. Furthermore, a variety of FACTS devices can be incorporated in the redispatching problem to enhance system security. Several case studies based on the IEEE 24-bus system and on a real size model of the Italian system are analysed and discussed.

1 Introduction

1.1 Motivation

Most European day-ahead electricity markets provide dispatch solutions that are based on economic grounds and, generally, do not explicitly consider security issues. Then, the system operator must check system security and implement redispatching actions if needed. This paper provides an OPF-based security-driven redispatching procedure to assist the system operator to ensure an appropriate level of security. The proposed procedure is motivated by congestion management practice in mainland Spain [1], but can be easily extended to any security redispatching drawn by independent system operators (ISO) once market results are available.

1.2 Literature review

While ensuring an appropriate level of security within the above framework, the ISO should determine the minimal changes in the day-ahead market results that ensure a secure operation. Most of the procedures proposed in the literature consist in enforcing transmission capacity limits that are computed off-line to ensure stability conditions [2–5]. The use of these 'artificial' stability limits results normally in economic inefficiencies. In [6–10], the authors include online conditions based on the power flow equations that guarantee not only a stable operating point but also an *adequate* distance to a maximum loading condition associated with bus voltage limits, equipment thermal limits and/or the system voltage stability limits. In [6], the objective function is to maximise the distance to voltage collapse. Reference [7] provides a multi-objective procedure for solving an economic dispatch problem, whereas [8] and [9] provide a multi-objective market-clearing procedure. In these models, the objective function includes cost as well as other terms. Reference [10] provides an iterative model that combines the OPF and the Continuation Power Flow techniques (CPF). The formulation used in the present paper extends and enhances that in [11], where the authors propose a congestion management procedure that includes security and stability limits avoiding non-thermal line capacity constraints. The proposed model optimises a cost function and does not attempt to maximise the distance from the critical point (as in [10]), but ensures that the current dispatch solution has a sufficient security margin and that, if a contingency occurs, the system is still able to reach a stable state within the considered time horizon. Most papers considering OPF techniques and including voltage stability constraints [6–10] do not take into account the generation limits for the maximum loading condition. In [11], the authors address this issue by means of an iterative process. The tool developed in this paper includes generation limits directly, thus avoiding iterations.

In this paper, we include FACTS devices in the OPF problem. In particular, we consider the static model of four

FACTS devices, namely, the on-load tap-changer (LTC), the phase-shifting (PHS) transformer [12], the static var compensator (SVC) [13] and the thyristor-controlled series compensator (TCSC) [14]. FACTS have been effectively used in several OPF problems to reduce congestion [15–17], enhance security [18] and reduce generation costs [19]. An evaluation of the value of FACTS devices in the context of liberalised electricity markets is given in [20, 21]. The procedure developed in this paper allows incorporating FACTS devices in the context of security redispatching. Since generator turbine governors and certain FACTS devices do not respond instantaneously to disturbances but are subject to ramping while changing operating conditions, ramping limits are taken into account to ensure the desired loading margin (security level). Conversely, if a loading margin is imposed, ramping constraints inherent to component functioning result in higher rescheduling costs. Generator and FACTS ramping constraints are incorporated in this paper to ensure the desired loading margin within a given time framework.

1.3 Tool features

The proposed tool can be used to ensure an appropriate loading margin that allows avoiding voltage collapse problems even if the outage of any relevant transmission line/transformer occurs. The tool considers a full ac model of the network, as well as detailed static models of its different components, and represents the actual operating condition as well as a highly stressed one that simulates a load increase under line outage. Different types of FACTS devices are included in the network model to facilitate attaining the desired level of security. Security achievement is analysed with and without FACTS devices. The proposed procedure results in a number of corrective redispatching actions that achieve the desired level of security at minimum cost using the available control devices in the network.

1.4 Contributions

The contributions of this paper are the development of:

1. a short-term OPF-based security-driven redispatching tool that is computationally efficient and robust;

2. a redispatching tool that can accommodate any type of FACTS devices to enhance security;

3. a procedure that simultaneously considers two operating conditions, the actual one and a stressed condition that guarantees a pre-specified level of security, while incorporating a set of ramping constraints that ensure that the stressed condition can be reached.

2 List of symbols

The notation used throughout the paper is stated below for quick reference. The symbol ' ˆ ' indicates the stressed condition.

2.1 Functions

$I_{nm}(\cdot)$ current magnitude from bus n to bus m as a function of the state variables

$P_{nm}(\cdot)$ active power flow from bus n to bus m as a function of the state variables

$Q_{nm}(\cdot)$ reactive power flow from bus n to bus m as a function of the state variables

2.2 Variables

$b_{\mathrm{SVC},n}$ susceptance of the SVC device at bus n

$P_{\mathrm{D}i}$ active power consumption of demand i

$P_{\mathrm{D}n}$ total active power consumption at bus n

$P_{\mathrm{G}j}$ active power production of generator j

$P_{\mathrm{G}n}$ total active power production at bus n

$Q_{\mathrm{D}n}$ total reactive power consumption at bus n

$Q_{\mathrm{G}j}$ reactive power production of generator j

$Q_{\mathrm{G}n}$ total reactive power production at bus n

$Q_{\mathrm{SVC},n}$ reactive power injected by the SVC device at bus n

T_k tap ratio of LTC k

V_n voltage magnitude at bus n

$x_{\mathrm{TCSC},k}$ reactance of the TCSC device connected to line k

$\Delta P_{\mathrm{D}i}^{\mathrm{down}}$ active power decrease in demand i for security purposes

$\Delta P_{\mathrm{D}i}^{\mathrm{up}}$ active power increase in demand i for security purposes

$\Delta P_{\mathrm{G}j}^{\mathrm{down}}$ active power decrease in generator j for security purposes

$\Delta P_{\mathrm{G}j}^{\mathrm{up}}$ active power increase in generator j for security purposes

θ_n voltage angle at bus n

ϕ_k phase of the PHS transformer k

2.3 Constants

$b_{\mathrm{SVC},n}^{\mathrm{max}}$ maximum susceptance of the SVC at bus n

$b_{\mathrm{SVC},n}^{\mathrm{min}}$ minimum susceptance of the SVC at bus n

$I_{\mathrm{TH},k}^{\mathrm{max}}$ maximum current magnitude of element k

$P_{\mathrm{D}i}^{\mathrm{A}}$ active power consumed by demand i as determined by the day-ahead market-clearing procedure

IET Gener. Transm. Distrib., 2008, Vol. 2, No. 6, pp. 821–833
doi: 10.1049/iet-gtd:20080064

P_{Gj}^{A} active power produced by generator j as determined by the day-ahead market-clearing procedure
P_{Di}^{max} maximum power to be supplied to demand i
P_{Di}^{min} minimum power to be supplied to demand i
P_{Gj}^{max} maximum power output of generator j
P_{Gj}^{min} minimum power output of generator j
Q_{Gj}^{max} maximum reactive power limit of generator j
Q_{Gj}^{min} minimum reactive power limit of generator j
r_{Di}^{down} price offered by demand i to decrease its day-ahead power schedule for security purposes
r_{Di}^{up} price offered by demand i to increase its day-ahead power schedule for security purposes
r_{Gj}^{down} price offered by generator j to decrease its day-ahead power schedule for security purposes
r_{Gj}^{up} price offered by generator j to increase its day-ahead power schedule for security purposes
R_{Gj}^{up} ramp-up limit of generator j
R_{Gj}^{down} ramp-down limit of generator j
$R_{T_k}^{up}$ ramp-up limit of LTC transformer k
$R_{T_k}^{down}$ ramp-down limit of LTC transformer k
$R_{\phi_k}^{up}$ ramp-up limit of PHS transformer k
$R_{\phi_k}^{down}$ ramp-down limit of PHS transformer k
T_k^{max} maximum tap ratio of LTC transformer k
T_k^{min} minimum tap ratio of LTC transformer k
V_n^{max} maximum voltage magnitude of bus n
V_n^{min} minimum voltage magnitude of bus n
$x_{TCSC,k}^{max}$ maximum reactance of the TCSC at line k
$x_{TCSC,k}^{min}$ minimum reactance of the TCSC at line k
ϕ_k^{max} maximum phase-shifter tap of PHS transformer k
ϕ_k^{min} minimum phase-shifter tap of PHS transformer k
ψ_{Di} power factor angle of demand i

2.4 Parameters

b_k series susceptance of element k
b_{pk} shunt susceptance of element k
g_k conductance of element k
r_k resistance of element k
x_k reactance of element k
Δt time period
λ loading parameter

2.5 Sets

$\mathcal{D}$ set of demands
$\mathcal{D}_n$ set of demands located at bus n
$\mathcal{G}$ set of online generators
$\mathcal{G}_n$ set of online generators located at bus n
$\mathcal{N}$ set of buses
$\mathcal{N}_{SVC}$ set of buses with SVCs
Θ_n set of buses connected to bus n
Ω_L set of transmission lines
Ω_{LTC} set of LTC transformers
Ω_{PHS} set of PHS transformers
Ω_{TCSC} set of lines with TCSCs

3 Modelling of components

3.1 Transmission line

Transmission lines are modelled by the well-known equivalent π-circuit. The active and reactive power flows from bus n to bus m are, respectively

$$P_{nm}(\cdot) = V_n^2 g_k - V_n V_m (g_k \cos(\theta_n - \theta_m) + b_k \sin(\theta_n - \theta_m)), \quad \forall k = (n, m) \in \Omega_L \tag{1}$$

$$Q_{nm}(\cdot) = -V_n^2 (b_k + b_{pk}) - V_n V_m (g_k \sin(\theta_n - \theta_m) - b_k \cos(\theta_n - \theta_m)), \quad \forall k = (n, m) \in \Omega_L \tag{2}$$

and the current flow through the transmission line from n to m is

$$I_{nm}(\cdot) = ((-V_n b_{pk} \sin\theta_n + V_n(g_k \cos\theta_n - b_k \sin\theta_n) - V_m(g_k \cos\theta_m - b_k \sin\theta_m))^2 + (V_n b_{pk} \cos\theta_n + V_n(g_k \sin\theta_n + b_k \cos\theta_n) - V_m(g_k \sin\theta_m + b_k \cos\theta_m))^2)^{1/2}, \quad \forall k = (n, m) \in \Omega_L \tag{3}$$

3.2 On-load tap changer and phase-shifting transformers

The models of the LTC and the PHS transformers are based on [12]. If an LTC/PHS/fixed-tap transformer is connected between buses n and m and regulates the voltage/phase at bus m, the active and reactive power flows are, respectively

$$P_{nm}(\cdot) = V_n^2 g_k - T_k V_n V_m (g_k \cos(\theta_n - \theta_m - \phi_k) + b_k \sin(\theta_n - \theta_m - \phi_k)) \tag{4}$$

$$Q_{nm}(\cdot) = -V_n^2 b_k - T_k V_n V_m (g_k \sin(\theta_n - \theta_m - \phi_k) - b_k \cos(\theta_n - \theta_m - \phi_k)) \tag{5}$$

If the transformer regulates the voltage/phase at bus n, the active and reactive power flows are, respectively

$$P_{nm}(\cdot) = T_k^2 V_n^2 g_k - T_k V_n V_m (g_k \cos(\theta_n - \theta_m + \phi_k) + b_k \sin(\theta_n - \theta_m + \phi_k)) \quad (6)$$

$$Q_{nm}(\cdot) = -T_k^2 V_n^2 b_k - T_k V_n V_m (g_k \sin(\theta_n - \theta_m + \phi_k) - b_k \cos(\theta_n - \theta_m + \phi_k)) \quad (7)$$

where the sub-index k identifies the component in between buses n and m. The current flow through an LTC/PHS/fixed-tap transformer that regulates the voltage/phase at bus m is

$$I_{nm}(\cdot) = ((V_n(g_k \cos\theta_n - b_k \sin\theta_n) - T_k V_m(g_k \cos(\theta_m + \phi_k) - b_k \sin(\theta_m + \phi_k)))^2 + (V_n(g_k \sin\theta_n + b_k \cos\theta_n) - T_k V_m(g_k \sin(\theta_m + \phi_k) + b_k \cos(\theta_m + \phi_k)))^2)^{1/2} \quad (8)$$

and the current flow through an LTC/PHS/fixed-tap transformer that regulates the voltage/phase at bus n is

$$I_{nm}(\cdot) = ((T_k V_n(g_k \cos(\theta_n + \phi_k) - b_k \sin(\theta_n + \phi_k)) - V_m(g_k \cos\theta_m - b_k \sin\theta_m))^2 + (T_k V_n(g_k \sin(\theta_n + \phi_k) + b_k \cos(\theta_n + \phi_k)) - V_m(g_k \sin\theta_m + b_k \cos\theta_m))^2)^{1/2} \quad (9)$$

Equations (4)–(9) are valid for LTCs, PHSs and fixed-tap transformers as follows.

1. LTC: $k = (n, m) \in \Omega_{\text{LTC}}$, T_k is a variable and $\phi_k = 0$.

2. PHS: $k = (n, m) \in \Omega_{\text{PHS}}$, ϕ_k is a variable and T_k is a constant.

3. Fixed tap transformer: $k = (n, m) \in \Omega_l$, T_k is a constant and $\phi_k = 0$.

3.3 Static var compensator

SVC devices can be modelled as a variable shunt susceptance [13]. Hence, the reactive power injected by the SVC at bus n is

$$Q_{\text{SVC},n} = -b_{\text{SVC},n} V_n^2, \quad \forall n \in \mathcal{N}_{\text{SVC}} \quad (10)$$

3.4 Thyristor-controlled series compensator

The model of the TCSC used in this paper is a variable reactance connected in series with a transmission line [14]. That is

$$z_k = r_k + j(x_k + x_{\text{TCSC}}), \quad \forall k = (n, m) \in \Omega_{\text{TCSC}} \quad (11)$$

The resulting conductance and susceptance are, respectively

$$g_k = \frac{r_k}{r_k^2 + (x_k + x_{\text{TCSC}})^2}, \quad \forall k = (n, m) \in \Omega_{\text{TCSC}} \quad (12)$$

$$b_k = \frac{-(x_k + x_{\text{TCSC}})}{r_k^2 + (x_k + x_{\text{TCSC}})^2}, \quad \forall k = (n, m) \in \Omega_{\text{TCSC}} \quad (13)$$

4 Model description

This section describes in detail all constraints used in the proposed redispatching procedure.

4.1 Cost of power adjustments

The cost of power adjustments that ensures a secure operation is modelled as follows

$$z = \sum_{j \in \mathcal{G}} (r_{\text{G}j}^{\text{up}} \Delta P_{\text{G}j}^{\text{up}} + r_{\text{G}j}^{\text{down}} \Delta P_{\text{G}j}^{\text{down}}) + \sum_{i \in \mathcal{D}} (r_{\text{D}i}^{\text{up}} \Delta P_{\text{D}i}^{\text{up}} + r_{\text{D}i}^{\text{down}} \Delta P_{\text{D}i}^{\text{down}}) \quad (14)$$

Equation (14) establishes that any change from the operating condition obtained in the day-ahead market (base case) implies a payment to the agent involved. Note that alternative criteria can be used.

4.2 Power flow equations

The current operating condition is defined by the active and reactive power balance at all buses

$$P_{\text{G}n} - P_{\text{D}n} = \sum_{m \in \Theta_n} P_{nm}(\cdot), \quad \forall n \in \mathcal{N} \quad (15)$$

$$Q_{\text{G}n} - Q_{\text{D}n} = \sum_{m \in \Theta_n} Q_{nm}(\cdot), \quad \forall n \in \mathcal{N} \quad (16)$$

where the powers on the left-hand side of each equation are defined as

$$P_{\text{G}n} = \sum_{j \in \mathcal{G}_n} P_{\text{G}j}, \quad \forall n \in \mathcal{N} \quad (17)$$

$$P_{\text{D}n} = \sum_{i \in \mathcal{D}_n} P_{\text{D}i}, \quad \forall n \in \mathcal{N} \quad (18)$$

$$Q_{\text{G}n} = \sum_{j \in \mathcal{G}_n} Q_{\text{G}j}, \quad \forall n \in \mathcal{N} \quad (19)$$

$$Q_{\text{D}n} = \sum_{i \in \mathcal{D}_n} P_{\text{D}i} \tan(\psi_{\text{D}i}), \quad \forall n \in \mathcal{N} \quad (20)$$

and

$$P_{\text{G}j} = P_{\text{G}j}^{\text{A}} + \Delta P_{\text{G}j}^{\text{up}} - \Delta P_{\text{G}j}^{\text{down}}, \quad \forall j \in \mathcal{G} \quad (21)$$

$$P_{\text{D}i} = P_{\text{D}i}^{\text{A}} + \Delta P_{\text{D}i}^{\text{up}} - \Delta P_{\text{D}i}^{\text{down}}, \quad \forall i \in \mathcal{D} \quad (22)$$

doi: 10.1049/iet-gtd:20080064

where in (20) we assumed constant power factor loads. The functions on the right-hand side of (15) and (16) depend on the device:

1. Equations (1) and (2) correspond to transmission lines;

2. Equations (4) and (5) or (6) and (7) correspond to LTCs, PHSs and fixed-tap transformers, depending on the regulated bus;

3. Equations (1) and (2) with (12) and (13) correspond to transmission lines that incorporate TCSC devices and

4. Equation (10) has to be added to the right-hand side of (16) for SVC devices.

4.3 Power flow equations for the stressed condition

The power flow equations for the stressed loading condition are

$$\hat{P}_{\mathrm{G}n} - \hat{P}_{\mathrm{D}n} = \sum_{m\in\Theta_n} \hat{P}_{nm}(\cdot), \quad \forall n \in \mathcal{N} \tag{23}$$

$$\hat{Q}_{\mathrm{G}n} - \hat{Q}_{\mathrm{D}n} = \sum_{m\in\Theta_n} \hat{Q}_{nm}(\cdot), \quad \forall n \in \mathcal{N} \tag{24}$$

where the powers on the left-hand side of (23) and (24) are defined as

$$\hat{P}_{\mathrm{G}n} = \sum_{j\in\mathcal{G}_n} \hat{P}_{\mathrm{G}j}, \quad \forall n \in \mathcal{N} \tag{25}$$

$$\hat{P}_{\mathrm{D}n} = \sum_{i\in\mathcal{D}_n} (1+\lambda) P_{\mathrm{D}i}, \quad \forall n \in \mathcal{N} \tag{26}$$

$$\hat{Q}_{\mathrm{G}n} = \sum_{j\in\mathcal{G}_n} \hat{Q}_{\mathrm{G}j}, \quad \forall n \in \mathcal{N} \tag{27}$$

$$\hat{Q}_{\mathrm{D}n} = \sum_{i\in\mathcal{D}_n} (1+\lambda) P_{\mathrm{D}i} \tan(\psi_{\mathrm{D}i}), \quad \forall n \in \mathcal{N} \tag{28}$$

with $P_{\mathrm{D}i}$ defined in (22). To use a scalar loading margin λ is an arbitrary choice, as other models can be used, such as vectorial λ, that is, one loading margin for each load.

The functions of the right-hand side of (23) and (24) have the same expressions as (15) and (16), respectively, where the variables V_n, θ_n, T_k, ϕ_k, $x_{\mathrm{TCSC},k}$ and $b_{\mathrm{SVC},n}$ are replaced by $\hat{V}_n$, $\hat{\theta}_n$, $\hat{T}_k$, $\hat{\phi}_k$, $\hat{x}_{\mathrm{TCSC},k}$ and $\hat{b}_{\mathrm{SVC},n}$, respectively.

Equations (23)–(28) are introduced to represent the system at the loading level that is fixed by the loading parameter λ. This stressed loading point can be associated either to a voltage stability limit or to a hard limit. Voltage stability limits lead to a system collapse and correspond to a saddle-node bifurcation (system singularity) or to a limit-induced bifurcation (generator reactive power limit). Hard limits are voltage limits or transmission line thermal limits. These limits do not directly cause a collapse but should be avoided since they can initiate cascade line tripping phenomena.

To enforce the $N-1$ contingency criterion, (23)–(28) include the worst-line outage [8]. For the interested reader, a reference on how to determine the set of worst-case contingencies for voltage stability constrained OPF problems is [9]. This reference shows that the N-1 contingency criterion, which in principle requires the solution of a very large multi-contingency OPF problem, can be implemented efficiently by solving a reduced number of single-contingency OPF problems. Because of space limitations, but without loss of generality, we only show the results for the most critical contingency. However, for each case study, we have ranked contingencies and considered the set of worst-case contingencies as explained in [9].

4.4 Demand limits

The demands are limited by minimum and maximum power bounds

$$P_{\mathrm{D}i}^{\min} \le P_{\mathrm{D}i} \le P_{\mathrm{D}i}^{\max}, \quad \forall i \in \mathcal{D} \tag{29}$$

4.5 Physical limits

The power production is limited by the capacity of the generators. Hence, under normal and stressed conditions

$$P_{\mathrm{G}j}^{\min} \le P_{\mathrm{G}j} \le P_{\mathrm{G}j}^{\max}, \quad \forall j \in \mathcal{G} \tag{30}$$

$$P_{\mathrm{G}j}^{\min} \le \hat{P}_{\mathrm{G}j} \le P_{\mathrm{G}j}^{\max}, \quad \forall j \in \mathcal{G} \tag{31}$$

$$Q_{\mathrm{G}j}^{\min} \le Q_{\mathrm{G}j} \le Q_{\mathrm{G}j}^{\max}, \quad \forall j \in \mathcal{G} \tag{32}$$

$$Q_{\mathrm{G}j}^{\min} \le \hat{Q}_{\mathrm{G}j} \le Q_{\mathrm{G}j}^{\max}, \quad \forall j \in \mathcal{G} \tag{33}$$

Bus voltages of the system under normal and stressed conditions must be within operating limits

$$V_n^{\min} \le V_n \le V_n^{\max}, \quad \forall n \in \mathcal{N} \tag{34}$$

$$V_n^{\min} \le \hat{V}_n \le V_n^{\max}, \quad \forall n \in \mathcal{N} \tag{35}$$

The current flow through all elements of the network must be below thermal limits

$$I_{nm}(\cdot) \le I_{\mathrm{TH},k}^{\max} \tag{36}$$

$$I_{mn}(\cdot) \le I_{\mathrm{TH},k}^{\max} \tag{37}$$

$$\hat{I}_{nm}(\cdot) \le I_{\mathrm{TH},k}^{\max} \tag{38}$$

$$\hat{I}_{mn}(\cdot) \le I_{\mathrm{TH},k}^{\max} \tag{39}$$

where the functions $I_{nm}(\cdot)$ and $I_{mn}(\cdot)$ are defined by (3) for transmission lines and by (8) and (9) for LTC, PHS and fixed-tap transformers. If a TCSC device is connected to a transmission line, the expression of the current flow is (3)

where the parameters g_k and b_k are defined by (12) and (13), respectively. Flows from m to n are not exactly equal to flows from n to m because of losses. The functions $\hat{I}_{nm}(\cdot)$ and $\hat{I}_{mn}(\cdot)$ have the same expressions as $I_{nm}(\cdot)$ and $I_{mn}(\cdot)$ but changing the corresponding variables to those pertaining to the stressed loading condition.

The changes in the production of generators are limited by ramp constraints

$$\hat{P}_{\mathrm{G}j} - P_{\mathrm{G}j} \leq R_{\mathrm{G}j}^{\mathrm{up}} \Delta t, \quad \forall j \in \mathcal{G} \tag{40}$$

$$P_{\mathrm{G}j} - \hat{P}_{\mathrm{G}j} \leq R_{\mathrm{G}j}^{\mathrm{down}} \Delta t, \quad \forall j \in \mathcal{G} \tag{41}$$

The time interval Δt is the time duration within which power productions have to be adjusted in order to guarantee the desired security margin. Observe also that (40) and (41) along with (26) and (28) couple the variables of the stressed system with those pertaining to the current dispatch solution.

Constraints (40) and (41) enforce the fact that up and down variations of generated powers can be obtained only within given rates, which in turn depends on the type and the characteristics of the power plants. These constraints ensure that the stressed operating point can be reached within the time duration considered and in case that the worst contingency occurs. Since the stressed operating point is stable, an adequate security level is ensured.

While the response of SVC and TCSC devices to apply required changes can be considered instantaneous for the considered time duration Δt, the response of the LTC and PHS is conditioned by a mechanically driven operation and it is not instantaneous. As for generators, these physical constraints relate to ramp limits

$$\hat{T}_k - T_k \leq R_{\mathrm{T}}^{\mathrm{up}} \Delta t, \quad \forall k = (n, m) \in \Omega_{\mathrm{LTC}} \tag{42}$$

$$T_k - \hat{T}_k \leq R_{\mathrm{T}}^{\mathrm{down}} \Delta t, \quad \forall k = (n, m) \in \Omega_{\mathrm{LTC}} \tag{43}$$

$$\hat{\phi}_k - \phi_k \leq R_{\phi}^{\mathrm{up}} \Delta t, \quad \forall k = (n, m) \in \Omega_{\mathrm{PHS}} \tag{44}$$

$$\phi_k - \hat{\phi}_k \leq R_{\phi}^{\mathrm{down}} \Delta t, \quad \forall k = (n, m) \in \Omega_{\mathrm{PHS}} \tag{45}$$

These constraints within the proposed security redispatching model constitute a contribution of the paper.

Note that we implicitly assume that the redispatching actions, such as power adjustments and FACTS operations, are feasible within the time duration Δt.

Finally, any device connected to the system is allowed to vary within design rating values. Therefore under normal and stressed conditions, for LTCs

$$T_k^{\min} \leq T_k \leq T_k^{\max}, \quad \forall k = (n, m) \in \Omega_{\mathrm{LTC}} \tag{46}$$

$$T_k^{\min} \leq \hat{T}_k \leq T_k^{\max}, \quad \forall k = (n, m) \in \Omega_{\mathrm{LTC}} \tag{47}$$

for PHSs

$$\phi_k^{\min} \leq \phi_k \leq \phi_k^{\max}, \quad \forall k = (n, m) \in \Omega_{\mathrm{PHS}} \tag{48}$$

$$\phi_k^{\min} \leq \hat{\phi}_k \leq \phi_k^{\max}, \quad \forall k = (n, m) \in \Omega_{\mathrm{PHS}} \tag{49}$$

for TCSCs

$$x_{\mathrm{TCSC},k}^{\min} \leq x_{\mathrm{TCSC},k} \leq x_{\mathrm{TCSC},k}^{\max}, \quad \forall k = (n, m) \in \Omega_{\mathrm{TCSC}} \tag{50}$$

$$x_{\mathrm{TCSC},k}^{\min} \leq \hat{x}_{\mathrm{TCSC},k} \leq x_{\mathrm{TCSC},k}^{\max}, \quad \forall k = (n, m) \in \Omega_{\mathrm{TCSC}} \tag{51}$$

and for SVCs

$$b_{\mathrm{SVC},n}^{\min} \leq b_{\mathrm{SVC},n} \leq b_{\mathrm{SVC},n}^{\max}, \quad \forall n \in \mathcal{N}_{\mathrm{SVC}} \tag{52}$$

$$b_{\mathrm{SVC},n}^{\min} \leq \hat{b}_{\mathrm{SVC},n} \leq b_{\mathrm{SVC},n}^{\max}, \quad \forall n \in \mathcal{N}_{\mathrm{SVC}} \tag{53}$$

Limits of FACTS devices are of two kinds: (i) technical operating limits, such as tap ratio and phase limits (46)–(49), and (ii) capacity limits, such as reactance sizes of the TCSCs (50) and (51) and susceptance sizes of the SVCs (52) and (53). While technical operating limits do not generally condition the device cost, capacity limits are directly related to the cost of the devices and, in turn, condition the planning strategy of the transmission network.

4.6 Other constraints

The proposed OPF problem is completed with the following additional constraints

$$-\pi \leq \theta_n \leq \pi, \quad \forall n \in \mathcal{N} \tag{54}$$

$$-\pi \leq \hat{\theta}_n \leq \pi, \quad \forall n \in \mathcal{N} \tag{55}$$

$$\theta_{\mathrm{ref}} = 0 \tag{56}$$

$$\hat{\theta}_{\mathrm{ref}} = 0 \tag{57}$$

4.7 Problem formulation

The formulation of the OPF-based security-driven short-term redispatching procedure is summarised below

Minimise (14)

subject to

1. power flow equations under the normal loading condition (15) and (16);

doi: 10.1049/iet-gtd:20080064

2. power flow equations under the stressed loading condition (23) and (24);

3. demand limits (29);

4. physical limits (30)–(53) and

5. other constraints (54)–(57).

4.8 Cost allocation of power adjustment

In order to recover the cost of the power adjustments resulting from the solution of (14)–(57), a *pro rata* method for sharing the costs of this security redispatch can be used. The cost per MW of power adjustment is

$$p = \frac{z^*}{\sum P_{Gj} + \sum P_{Di}} \tag{58}$$

Since all users of the network benefit from the security improvement, each user pays an amount proportional to its actual power production or consumption, that is, $p \cdot P_{Gj}$ and $p \cdot P_{Di}$, respectively. Other methods for distributing costs can be considered, but a discussion on this point is beyond the scope of the paper.

5 Case study

In this section, the proposed security-driven redispatching procedure is applied to the IEEE 24-bus Reliability Test System (IEEE RTS) and to a real-size 129-bus model of the Italian system. Problem (14)–(57) is a non-convex one, thus no NLP solver can generally guarantee to find the global optimum. However, using different starting points, no different solutions were found. Thus, the solutions provided in the paper are feasible and appropriate from both the economical and the technical point of views. OPF results are obtained using MATLAB [22] and GAMS-CONOPT [23] that is a suitable solver for nonlinear programming problems. Note that CONOPT is one of the state-of-the-art NLP solvers. The simulations take about 1 s on a Sun Fire V20Z with two processors clocking at 2.40 GHz and 8 GB of RAM memory for the 24-bus test case and less than 3 min for the 129-bus network. The convergence tolerance of the objective function is $9 \cdot 10^{-8}$.

5.1 IEEE RTS case study

Fig. 1 depicts the 24-bus system that is fully described in [24]. In order to take into account the effect of FACTS on the redispatching procedure, the thermal limit of lines 11–13 is set to 1.75 p.u. Furthermore, we consider the outage of the transformer between buses 3 and 24 to force system congestion. This is the worst contingency for the 24-bus system. The time interval is $\Delta t = 5$ min. The costs of power adjustments and ramp constraints are provided in Appendix. Observe that generator costs are lower than

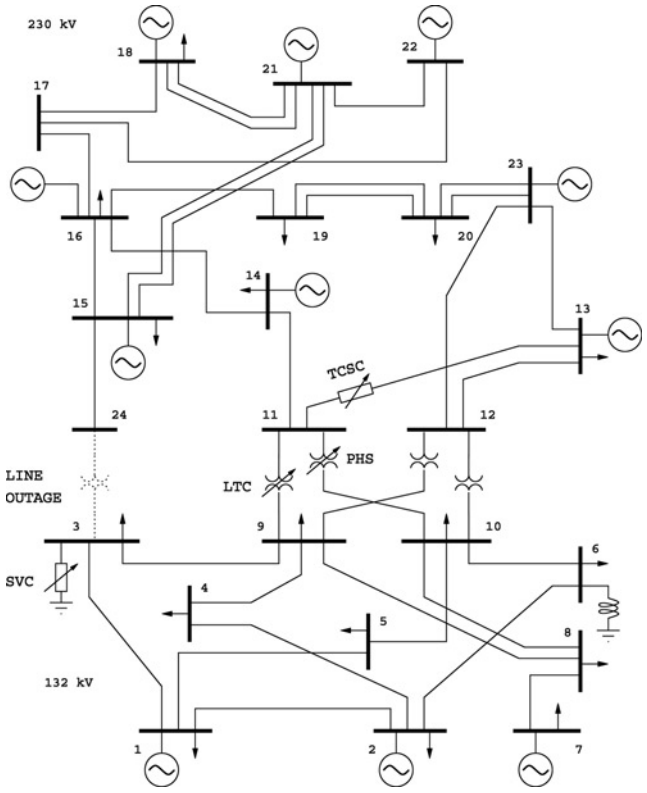

Figure 1 *24-bus test system (IEEE one area RTS-96 [24])*

demand costs. This implicitly means that loads are inelastic as long as the system can redistribute the generation; however, loads can be shed to maintain system security if the system is highly congested. Observe also that loads are allowed to increase, although the situation for which an inductive load improves system loadability by increasing its demand is unlikely. FACTS positions and other data are provided in Appendix.

We do not attempt to propose a method to determine the optimal placement of FACTS devices (a technique for optimal FACTS device placement can be found in [25]). The positions of FACTS devices have been selected based on the knowledge of the network and with the aim of improving the system loadability and security.

In the simulations below, each FACTS device is studied separately in order to better understand its effect on the redispatching procedure.

Problem (14)–(57) is certainly feasible for $\lambda = 0$, because the condition $\lambda = 0$ corresponds to the initial market solution (adjusted for losses). Problem (14)–(57) is also assumed to be feasible for all $N-1$ contingencies, which is a security criterion normally required in actual systems. However, as the loading parameter λ increases, (14)–(57) may become infeasible because the desired value of λ cannot be satisfied. Nevertheless, since the loading parameter is increased at each step by 1%, if the solution is

infeasible at a given step, say $i+1$, λ_i is the maximum loading condition with an error smaller than 1%.

Simulations results are depicted in Fig. 2. The curves represent the objective function z, namely the cost of power adjustments, as a function of the loading parameter λ. For $\lambda \leq 4\%$, no power adjustment is needed, thus the resulting cost is zero. For $\lambda > 4\%$, some power adjustments are needed to maintain the desired level of security. For $\lambda > 16\%$, the OPF problem for the system without FACTS devices becomes infeasible. As expected, the case without FACTS devices leads to the most expensive solutions as the value of λ increases. For $4\% \leq \lambda \leq 10\%$, the binding constraints are mainly voltage limits (in particular, at bus 3). For these values of the loading parameter, the most effective FACTS devices are the LTC and the SVC, which is reasonable, since these devices control voltage levels. On the other hand, for $4\% \leq \lambda \leq 10\%$, the effects of the PHS and the TCSC devices are negligible since there is no need of modifying power flows. For $\lambda > 10\%$, the binding constraints are mainly the limits on transmission lines (in particular, on line 11–13). An increasing amount of load has to be shed for these values of the loading parameter, hence the change in the slope of the cost z. The most effective FACTS devices are the PHS and the TCSC, circumstance that is to be expected because these devices best control power flows. For $\lambda > 10\%$ the effects of the LTC and the SVC are negligible because there is no voltage problem.

For the sake of illustration, we further discuss two snapshots of the solutions shown in Fig. 2, one for $\lambda = 8\%$ and another one for $\lambda = 14\%$. Furthermore, we show an example that combines two FACTS devices.

5.1.1 Solution for $\lambda = 8\%$: Fig. 3 depicts the generated powers at each bus and generator power adjustments for $\lambda = 8\%$. Power adjustments are in p.u. with respect to the base-case level. The bar chart shows the solution obtained without FACTS devices and with LTC and SVC devices. The base case solution (i.e. $\lambda = 0$) is also shown in Fig. 3. Solutions with PHS and TCSC are not depicted because these devices have no effect for this loading level. Only generators 13 and 22 are forced to reschedule their power production due to ramp limit constraints.

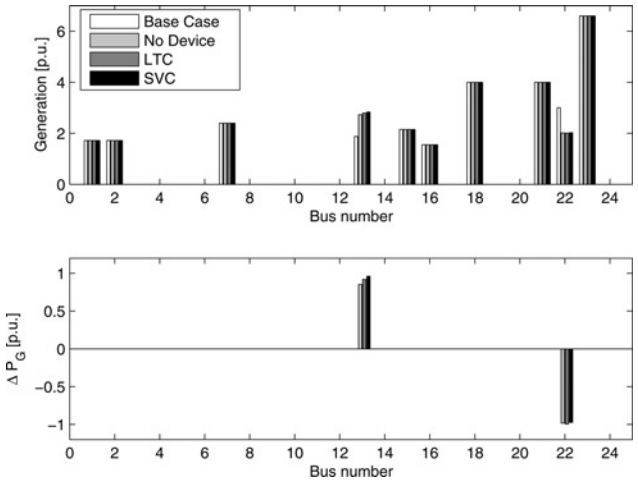

Figure 3 *Generated powers and generator power adjustments for $\lambda = 8\%$*
Effect of LTC and SVC devices for the 24-bus system

Fig. 4 depicts the power demands at each bus and demand power adjustments. The load to be shed is located at bus 3.

Table 1 provides the effects of FACTS devices in the total generation, the total generation adjustment, the total demand, the total demand adjustment, the total cost and the per-unit cost for the 24-bus system and $\lambda = 8\%$. Only the LTC and SVC devices are able to significantly reduce the cost and the amount of power adjustments.

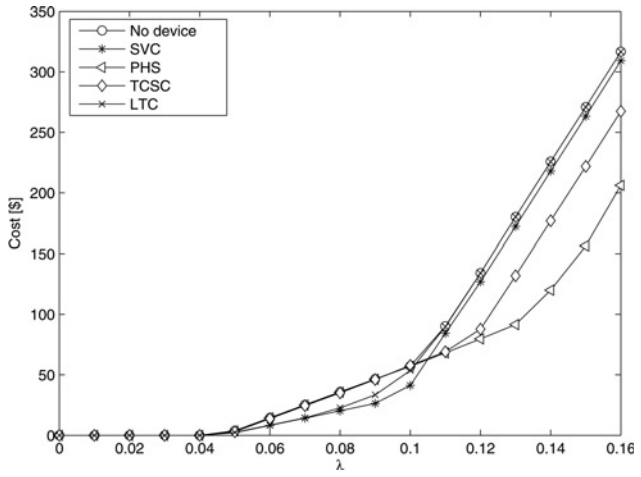

Figure 2 *Costs of power adjustments as a function of the loading parameter λ for the 24-bus system*
Effect of LTC, PHS, SVC and TCSC devices

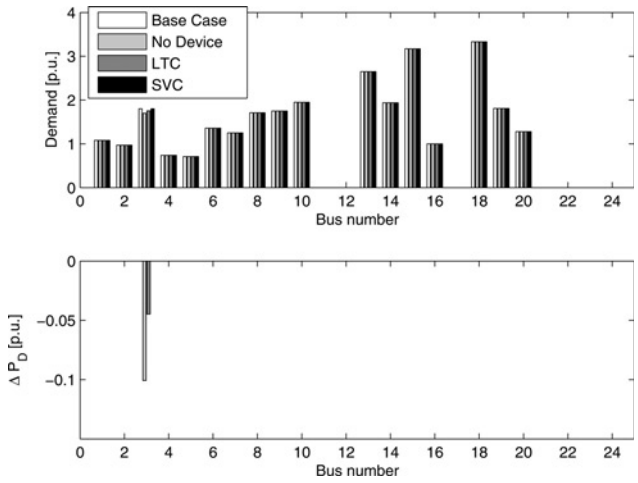

Figure 4 *Demand powers and load power adjustments for $\lambda = 8\%$*
Effect of LTC and SVC devices for the 24-bus system

doi: 10.1049/iet-gtd:20080064

Table 1 Total generation, total generation adjustment, total demand, total demand adjustment, total cost and per-unit cost for $\lambda = 8\%$

Device	Total generation, p.u.	$\sum_{j\in\mathcal{G}} \Delta P_{Gj}^{up}$, p.u.	$\sum_{j\in\mathcal{G}} \Delta P_{Gj}^{down}$, p.u.	Total demand, p.u.	$\sum_{i\in\mathcal{D}} \Delta P_{Di}^{down}$, p.u.	Total cost, $	Uplift cost, $/p.u.
No device	28.9104	0.8785	0.9840	28.4223	0.0777	35.8705	0.6257
LTC	28.9872	0.9583	0.9870	28.4890	0.0110	22.6318	0.3938
PHS	28.9193	0.8796	0.9762	28.4233	0.0767	35.6463	0.6216
SVC	28.9683	0.9587	1.0062	28.5000	0	20.2800	0.3529
TCSC	28.8997	0.8848	1.0010	28.4263	0.0737	35.1387	0.6130

However, with the SVC, there is no need of load shedding; thus, in this case, the SVC is more effective than the LTC. This result is mainly due to the position of the SVC in the network.

5.1.2 Solution for $\lambda = 14\%$: Fig. 5 illustrates the generated powers at each bus and generator power adjustments for $\lambda = 14\%$. Once again, power adjustments are in p.u. with respect to the base-case level. The bar chart shows the solution obtained without FACTS devices and with PHS and TCSC devices. The base-case solution (i.e. $\lambda = 0$) is also shown in Fig. 5. Solutions with LTC and SVC are not depicted because these devices have a small effect on cost for this loading level. In this case, only generators 13 and 22 are forced to reschedule their power production, mainly due to ramp limit constraints.

Fig. 6 depicts the power demands at each bus and the demand power adjustments. Owing to the higher loading level, the number of loads affected by shedding and the

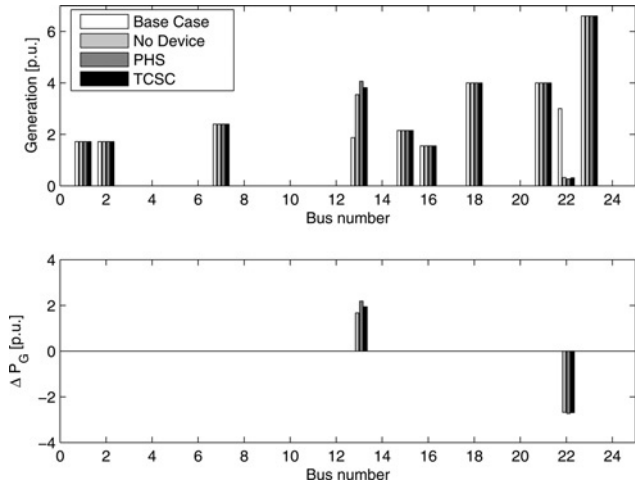

Figure 5 *Generated powers and generator power adjustments for $\lambda = 14\%$*

Effects of PHS and TCSC devices for the 24-bus system

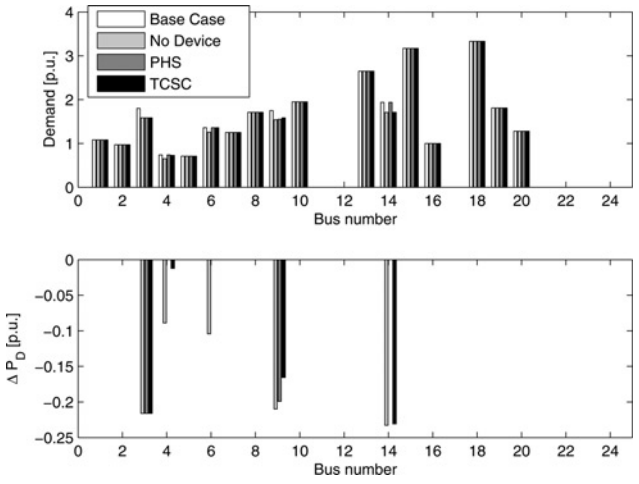

Figure 6 *Demand powers and load power adjustments for $\lambda = 14\%$*

Effect of PHS and TCSC devices for the 24-bus system

Table 2 Total generation, total generation adjustment, total demand, total demand adjustment, total cost and per-unit cost for $\lambda = 14\%$

Device	Total generation, p.u.	$\sum_{j\in\mathcal{G}} \Delta P_{Gj}^{up}$, p.u.	$\sum_{j\in\mathcal{G}} \Delta P_{Gj}^{down}$, p.u.	Total demand, p.u.	$\sum_{i\in\mathcal{D}} \Delta P_{Di}^{down}$, p.u.	Total cost, $	Uplift cost, $/p.u.
No device	28.0261	1.6851	2.6749	27.6661	0.8339	225.7398	4.0534
LTC	28.0359	1.6876	2.6676	27.6665	0.8335	225.6657	4.0513
PHS	28.5712	2.3059	2.7506	28.1857	0.3143	119.9716	2.1138
SVC	28.0493	1.7226	2.6892	27.6937	0.8063	217.9130	3.9092
TCSC	28.2750	1.9665	2.7070	27.9009	0.5991	176.8899	3.1489

total amount of load shedding is much higher than in the case of $\lambda = 8\%$.

Table 2 provides the effects of FACTS devices in the total generation, the total generation adjustment, the total demand, the total demand adjustment, the total cost and the per-unit cost for the 24-bus system and $\lambda = 14\%$. Only PHS and TCSC devices are able to significantly reduce the cost and the amount of power adjustment. However, the PHS leads to less expensive results than the TCSC. This is basically due to the fact that the TCSC device reaches its control limits.

Table 3 shows the total cost incurred using different control limits of FACTS devices. The first column indicates the factor used to reduce or increase FACTS limits. The results show that, for the considered case and with the given FACTS device positions, only the TCSC size significantly affects total costs for $\lambda = 14\%$. In general, we can conclude that the proposed tool is also effective for understanding the effect of the size of FACTS devices on the security redispatch.

5.1.3 Effect of FACTS ramping constraints: Ramping constraints that regulate the functioning of LTC and PHS devices basically affect the set point of bus voltage levels and generator reactive power productions as well as the FACTS controllable variables, that is, tap ratio T_k and phase-shifting angle ϕ_k. Table 4 shows the values of T_k and ϕ_k for the two considered loading levels, $\lambda = 8\%$ and $\lambda = 14\%$, respectively. The table also shows the values of FACTS controllable variables without ramp constraints. Observe that without the ramping constraints the system could not properly operate in case of the worst contingency.

Table 3 Total cost with different control limits of FACTS devices

Factor	$\lambda = 8\%$		$\lambda = 14\%$	
	SVC, $	TCSC, $	SVC, $	TCSC, $
0.1	23.3325	36.5586	222.8060	220.6598
0.5	20.3787	35.8839	220.2388	200.9769
1	20.2800	35.1387	217.9130	176.8899
2	20.1930	34.4942	215.0598	130.9531
10	20.1751	34.3448	214.9511	119.0912

Observe also that ramping constraints do not affect the cost of redispatching, since these constraints basically operate on variables such as voltage levels and reactive power productions that have no associated cost in the proposed OPF model.

5.1.4 Effect of combining multiple FACTS devices: As it has been discussed above, the effects of LTC and SVC devices (voltage-controlling devices) are basically decoupled from the effects of PHS and TCSC (power-flow-controlling devices). This fact suggests that the combined usage of one voltage-controlling device and a power-flow-controlling one can lead to comparatively cheaper solutions for all the range of load levels than other combinations. This is confirmed in Fig. 7. Because of system nonlinearities, combining two FACTS devices leads to an overall lower cost than the linear combination of each device, especially for $\lambda > 10\%$.

5.2 Case study based on the 129-bus Italian system

The proposed method is applied to a real-size 129-bus model of the Italian electric energy system. Most data of this system can be found in [26] and the time interval is $\Delta t = 3$ min. Because of space limitations, only the SVC and the TCSC devices are considered. The SVC is placed at bus Travagliato, while the TCSC is installed

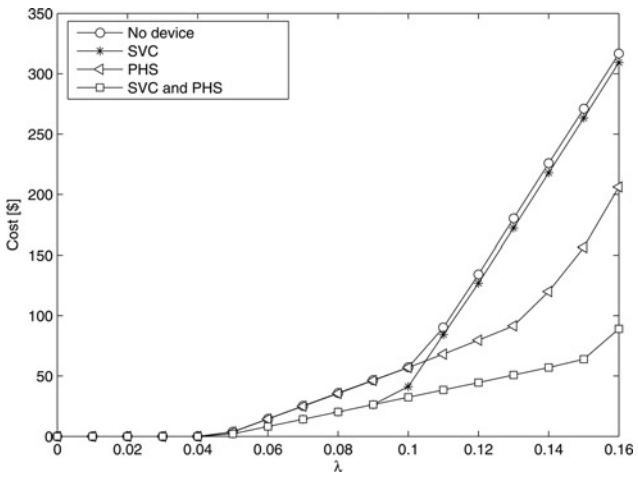

Figure 7 *Cost of power adjustments as a function of the load level λ for the 24-bus system*

Simultaneous effect of PHS and SVC devices

Table 4 Effects of ramping constraints on LTC and PHS variables

FACTS device	Variable	$\lambda = 8\%$		$\lambda = 14\%$	
		No ramps	With ramps	No ramps	With ramps
LTC	T	0.95	1.05	0.95	1.016
PHS	ϕ	−0.2618	0.0136	−0.2618	−0.1483

doi: 10.1049/iet-gtd:20080064

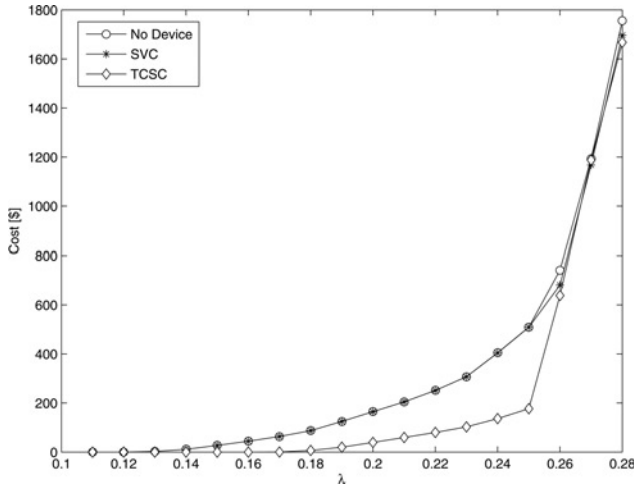

Figure 8 *Cost of power adjustments as a function of the load level λ for the 129-bus Italian system*
Effect of SVC and TCSC devices

on the HV line that connects buses Bovisio and Turbigo. All these buses are within the heavily loaded industrial area of Milan and have been selected based on the knowledge of the network and on feasibility considerations.

This area is not particularly weak since it is well interconnected to the rest of the Northern Italian HV grid and to the European HV grid through Switzerland. Thus, to force congestion, the transmission line in between buses Cagno and Musignano has been removed in the power flow equations under the stressed loading condition.

Fig. 8 shows the simulations results for the system without FACTS devices, with the SVC and with the TCSC. The curves represent the objective function z, namely the cost of power adjustments, as a function of the loading parameter λ. For $\lambda > 28\%$, the OPF problem for the system without FACTS devices becomes infeasible.

Observe that, despite the high load level, the voltage support provided by the SVC does not reduce the cost of power adjustments of the Italian grid. On the other hand, the TCSC is able to reduce the cost since a redistribution of power flows allows reducing congestion of transmission lines.

6 Conclusions

This paper presents a security-constrained redispatching model that is able to resolve system congestion and security issues. It is intended to help system operators to ensure an appropriate level of security once the market results are available. The model includes voltage stability constraints and generator ramp limits. It may include four types of FACTS devices, namely LTC, PHS, SVC and TCSC. Time delays of LTC and PHS devices are modelled as ramp limits of the controlled tap ratio and phase angle, respectively.

The effect of FACTS devices on the redispatching procedure is simulated and discussed in detail using the IEEE 24-bus system and a real-size model of the Italian electric energy system.

From the analysis carried out, it becomes apparent that the cost of power adjustments resulting from the proposed redispatching procedure can be reduced if adequate FACTS devices are installed in the system. This is not a surprising result; however, the proposed tool provides a precise and quantitative analysis of the effect of FACTS devices on the security redispatching.

The comparison of the results for different FACTS devices also shows that the proposed technique can be used as a planning tool. In fact, market participants may be interested in improving the system stability and security by asking the system operator to install FACTS devices. The number and the type of the devices to be installed can be determined based on their purchase and installation costs and the amount saved once FACTSs are installed. Future work will concentrate on the economic appraisal of FACTS devices and on the implementation of the power adjustments obtained with the proposed tool.

7 References

[1] CONEJO A.J.: 'The electricity market of mainland Spain: a brief critical review'. Proc. IEEE PES General Meeting, Tampa, Florida, 2007

[2] GEDRA T.W.: 'On transmission congestion and pricing', *IEEE Trans. Power Syst.*, 1999, **14**, (1), pp. 241–248

[3] BOLTON M.A., HILL D.J., KAYE R.J.: 'Designing ancillary services markets for power system security', *IEEE Trans. Power Syst.*, 2000, **15**, (2), pp. 675–680

[4] XIE K., SONG Y.-H., STONHAM J., YU E., LIU G.: 'Decomposition model and interior point methods for optimal spot pricing of electricity in deregulation environments', *IEEE Trans. Power Syst.*, 2000, **15**, (1), pp. 39–50

[5] BOMPARD E., CORREIA P., GROSS G., AMALIN M.: 'Congestion management schemes: a comparative analysis under a unified framework', *IEEE Trans. Power Syst.*, 2003, **18**, (1), pp. 346–352

[6] ROSEHART W., CAÑIZARES C.A., QUINTANA V.H.: 'Optimal power flow incorporating voltage collapse constraints'. Proc. IEEE PES Summer Meeting, Edmonton, Alberta, 1999

[7] ROSEHART W.D., CAÑIZARES C.A., QUINTANA V.: 'Multi-objective optimal power flows to evaluate voltage security costs in

power networks', *IEEE Trans. Power Syst.*, 2003, **18**, (2), pp. 578–587

[8] MILANO F., CAÑIZARES C.A., INVERNIZZI M.: 'Multi-objective optimization for pricing system security in electricity markets', *IEEE Trans. Power Syst.*, 2003, **18**, (2), pp. 596–604

[9] MILANO F., CAÑIZARES C.A., INVERNIZZI M.: 'Voltage stability constrained OPF market models considering $N-1$ contingency criteria', *Electric Power Syst. Res.*, 2005, **74**, (1), pp. 27–36

[10] MILANO F., CAÑIZARES C.A., CONEJO A.J.: 'Sensitivity-based security-constrained OPF market clearing model', *IEEE Trans. Power Syst.*, 2005, **20**, (4), pp. 2051–2060

[11] CONEJO A.J., MILANO F., GARCÍA-BERTRAND R.: 'Congestion management ensuring voltage stability', *IEEE Trans. Power Syst.*, 2006, **21**, (1), pp. 357–364

[12] ACHA E., AMBRIZ-PÉREZ H., FUERTE-ESQUIVEL C.R.: 'Advanced transformer control modeling in an optimal power flow using newton's method', *IEEE Trans. Power Syst.*, 2000, **15**, (1), pp. 290–298

[13] AMBRIZ-PÉREZ H., ACHA E., FUERTE-ESQUIVEL C.R.: 'Advanced SVC models for Newton–Raphson load flow and Newton optimal power flow studies', *IEEE Trans. Power Syst.*, 2000, **15**, (1), pp. 129–136

[14] FUERTE-ESQUIVEL C.R., ACHA E., AMBRIZ-PÉREZ H.: 'A thyristor controlled series compensator model for the power flow solution of practical power networks', *IEEE Trans. Power Syst.*, 2000, **15**, (1), pp. 58–64

[15] BERIZZI A., DELFANTI M., MARANNINO P., SAVINO M., SILVESTRI A.: 'Enhanced security-constrained OPF with FACTS devices', *IEEE Trans. Power Syst.*, 2005, **20**, (3), pp. 1597–1605

[16] HUG-GLANZMANN G., ANDERSSON G.: 'Incorporation of $N-1$ security into optimal power flow for facts control'. Proc. Power System Conference & Exposition (PSCE), Atlanta, Georgia, 2006

[17] SHAO W., VITTAL V.: 'LP-based OPF for corrective FACTS control to relieve overloads and voltage violations', *IEEE Trans. Power Syst.*, 2006, **21**, (4), pp. 1832–1839

[18] LEHMKÖSTER C.: 'Security Constrained optimal power flow for an economical operation of FACTS-devices in liberalized energy markets', *IEEE Trans. Power Deliv.*, 2002, **17**, (2), pp. 603–608

[19] PALMA-BEHNKE R., VARGAS L.S., PÉREZ J.R., NÚÑEZ J.D., TORRES R.A.: 'OPF with SVC and UPFC modeling for longitudinal systems' *IEEE Trans. Power Syst.*, 2004, **19**, (4), pp. 1742–1753

[20] SCHAFFNER C., ANDERSSON G.: 'Determining the value of controllable devices in a liberalized electricity market'. IEEE Power Tech, Bologna, Italy, 2003

[21] SCHAFFNER C., ANDERSSON G.: 'Valuating controllable devices in congested networks'. Proc. Bulk Power System Dynamics and Control VI Conf., Cortina d'Ampezzo, Italy, 2004

[22] The MathWorks, Inc.: 'MATLAB programming', http://www.mathworks.com, 2005

[23] Drud A.S. 'GAMS/CONOPT, GAMS. The solver manuals', http://www.gams.com/, 2005

[24] RELIABILITY TEST SYSTEM TASK FORCE OF THE APPLICATION OF PROBABILITY METHODS SUBCOMMITTEE: 'The IEEE Reliability Test System – 1996', *IEEE Trans. Power Syst.*, 1999, **14**, (3), pp. 1010–1020

[25] MÍNGUEZ R., MILANO F., ZÁRATE-MIÑANO R., CONEJO A.: 'Optimal network placement of SVC devices', *IEEE Trans. Power Syst.*, 2007, **21**, (4), pp. 1851–1860

[26] MILANO F.: 'Pricing system security in electricity market models with inclusion of voltage stability constraints'. PhD thesis, University of Genova, Genova, Italy, http://www.uclm.es/area/gsee/Web/Federico, 2003

8 Appendix

Tables 5 and 6 provide the cost of generation and demand power adjustments, respectively.

FACTS positions and data are as follows. Ramp constraint values are chosen based on typical time responses of LTC and PHS regulators.

1. The LTC connects buses 11 and 9. The maximum and minimum tap limits are $T^{\max} = 1.05$ p.u./p.u. and $T^{\min} = 0.95$ p.u./p.u., respectively, while ramp slopes are $R_{\mathrm{T}}^{\mathrm{up}} = 0.002$ p.u./p.u.min and $R_{\mathrm{T}}^{\mathrm{down}} = 0.002$ p.u./p.u.min.

2. The PHS transformer connects buses 11 and 10. The maximum and minimum phase angle limits are $\phi^{\max} = \pi/12$ rad and $\phi^{\min} = -\pi/12$ rad, respectively, while ramp slopes are $R_{\phi}^{\mathrm{up}} = \pi/600$ rad/min and $R_{\phi}^{\mathrm{down}} = \pi/600$ rad/min.

3. The SVC is placed at bus 3. The maximum and minimum susceptance limits are $b_{\mathrm{SVC}}^{\max} = 0.5$ p.u. and $b_{\mathrm{SVC}}^{\min} = -0.5$ p.u., respectively.

4. The TCSC is placed on the transmission line 11–13. The reactance maximum and minimum limits are $x_{\mathrm{TCSC}}^{\max} = 0.01$ p.u. and $x_{\mathrm{TCSC}}^{\min} = -0.01$ p.u., respectively.

doi: 10.1049/iet-gtd:20080064

Table 5 Per-unit cost of generation power adjustments

Generator number	Bus number	r_{Gj}^{down}, $/p.u.	r_{Gj}^{up}, $/p.u.	Generator number	Bus number	r_{Gj}^{down}, $/p.u.	r_{Gj}^{up}, $/p.u.
1	1	26	24	17	15	22	21
2	1	26	24	18	15	22	21
3	1	12	10	19	15	22	21
4	1	12	10	20	15	11	9
5	2	26	24	21	16	11	9
6	2	26	24	22	18	7	5
7	2	12	10	23	21	7	5
8	2	12	10	24	22	3	1
9	7	19	17	25	22	3	1
10	7	19	17	26	22	3	1
11	7	19	17	27	22	3	1
12	13	20	18	28	22	3	1
13	13	20	18	29	22	3	1
14	13	20	18	30	23	11	9
15	15	22	21	31	23	11	9
16	15	22	21	32	23	11	9

Table 6 Per-unit cost of demand power adjustments

Demand number	Bus number	r_{Di}^{down}, $/p.u.	r_{Di}^{up}, $/p.u.	Demand number	Bus number	r_{Di}^{down}, $/p.u.	r_{Di}^{up}, $/p.u.
1	1	220	200	10	10	230	210
2	2	220	200	11	13	220	230
3	3	220	200	12	14	220	200
4	4	230	210	13	15	210	190
5	5	230	210	14	16	210	190
6	6	230	210	15	18	210	190
7	7	240	210	16	19	220	190
8	8	240	220	17	20	210	190
9	9	230	200				

doi: 10.1049/iet-gtd:20080064